JOURNAL OF COMPUTATIONAL PHYSICS 36, 327–346 (1980)

Finite-Difference Methods for Computing the Steady Flow about Blunt Bodies

BERTIL GUSTAFSSON AND PER WAHLUND

Department of Computer Sciences, University of Uppsala, Sturegatan 4B 2 tr, Uppsala, Sweden

Received June 18, 1979; revised September 19, 1979

A numerical method for computation of the steady flow about a blunt body is presented. A difference scheme is applied on a domain which is such that the whole subsonic part is included. It is solved as a boundary-value problem with extrapolation conditions at the outflow boundary in the supersonic domain. The resulting system of algebraic equations is solved by a procedure of Newton. In the remaining supersonic domain a marching procedure is used.

1. INTRODUCTION

The problem of determining the bow shock shape and the gas flow around a blunt body traveling at supersonic speed has attained considerable interest for many years, as it has important applications, for example, in connection with supersonic flight and entry from space into the atmosphere. For this reason many computational methods have been developed for this problem. One possibility is to solve the inverse problem, where, from a prescribed shock and conditions across it one computes the state of the flow behind it and the body shape, e.g., as in the work of Lomax and Inouye [6]. Another commonly used method is to solve the time-dependent equations governing unsteady flow, obtaining the results for the steady flow asymptotically in time. Such a technique is used by Sutton [10] for computing the fully coupled radiating flow field around a blunt body. The so-called finite volume technique with a split explicit time differencing is used by Rizzi and Inouye [8] to compute both axisymmetric and fully three-dimensional blunt body flow.

A drawback with the time-dependent techniques is that they are often very time-consuming since the convergence to the steade state can be slow, and it can also be difficult to determine whether the steady state has been reached or not. We believe that a more efficient way is to solve the equations for steady flow directly as a boundary-value problem on a domain which contains the whole subsonic part of the flow. In the supersonic part of the domain we use a marching procedure in the main flow direction; see Fig. 1.

The system of equations arising from the difference approximation to the boundary-

0021-9991/80/090327-20$02.00/0

581/36/3-4

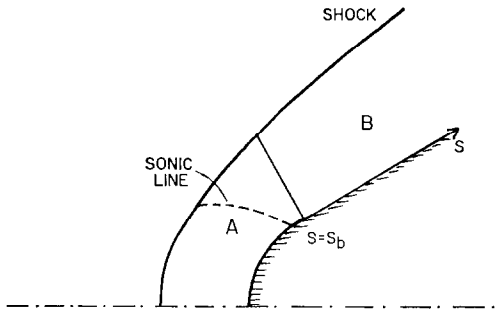

FIG. 1. Newton procedure in region A, marching procedure in region B.

value problem is solved by using Newton's method, and therefore we will refer to the solution method for this part as the Newton procedure.

The computations are made in a body-oriented coordinate system with the shock at a fixed coordinate value. The shock distance δ is treated in the same way as the other unknowns, which means that the variation of δ is determined by the Newton procedure in region A. The differential equations and coordinate transformations are described in Section 2.

The equations are approximated by second-order accurate centered difference approximations in the interior of the region A. This region contains part of the supersonic region, but the same difference method is used all over. This is a technique similar to that used by Blomster and Sköllermo [2]. At the shock values are given by the Rankine–Hugoniot relations and at the body the rigid-wall condition is applied. At the symmetry line we use the symmetry conditions, and at the outflow boundary of A extrapolation is used.

Gaussian elimination is used to solve the system of linear equations arising at each step of the iterative procedure. The complete treatment of region A is described in Section 3.

In region B, a dissipative version of the leap-frog scheme is used and the initial data are taken from the Newton calculation at the boundary between the regions. A variable step size is used, to allow for larger steps further downstream. The complete algorithm for region B is presented in Section 4.

The results of the numerical computation for different Mach numbers between 2 and 40 are presented in Section 5.

The method is applied to the perfect gas case, but the generalization is straightforward for more general cases, where radiative heating is also included. The efficiency of the method as indicated by our experiments is expected to be more pronounced for more general and more time-consuming cases.

The method is designed for fairly high Mach numbers such that the subsonic domain is finite. Furthermore, if the subsonic domain is very large such that the angle between the shock and the body becomes large, a different coordinate system should be used. Rizzi [9] has considered that problem.

2. The Differential Equations

We will consider inviscid, axisymmetric flow, which is homentropic in the domain of computation. The flow is governed by the equations of conservation of mass, momentum, and energy for unsteady flow. These conservation equations expressed in vector notation are

mass:

$$\frac{\partial \rho}{\partial t} + \nabla \cdot (\rho V) = 0, \tag{2.1}$$

momentum:

$$\frac{\partial V}{\partial t} + V \cdot \nabla V - V p/\rho = 0, \tag{2.2}$$

energy:

$$\rho \frac{\partial h}{\partial t} + \rho V \cdot \nabla h - \frac{\partial p}{\partial t} - V \cdot \nabla p = 0, \tag{2.3}$$

where V is the flow velocity vector, ρ the density, p the pressure, and h the enthalpy, i.e., energy per unit mass.

We are going to use the same formulation of the equations and the same coordinate systems that are used by Sutton [10], where the shock is assumed to be a smooth surface. The coordinate system is shown in Fig. 2.

The transformation of Eqs. (2.1)–(2.3) to this coordinate system is carried out in [10].

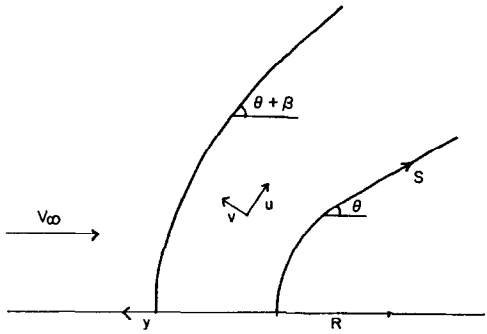

FIG. 2. The body-oriented coordinate system. s, Coordinate along body surface; y, coordinate perpendicular to body surface; ϕ, angle measured around symmetry axis (not shown); θ, angle between tangent to body and symmetry axis; $\theta + \beta$, angle between tangent to shock wave and symmetry axis; R, nose radius of body; u, flow velocity parallel to body; v, flow velocity perpendicular to body.

In order to fix the location of the shock wave in the coordinate system we introduce the shock stand-off distance $\delta = \delta(s, t)$ and make the coordinate transformation

$$y' = y/\delta. \tag{2.4}$$

We now have a rectangular coordinate system with $y' = 0$ at the body and $y' = 1$ at the shock. We will hereafter use the unprimed variable y to simplify writing. s is the distance from the symmetry axis along the body surface. With these transformations and assuming axisymmetric flow so that all derivatives and velocities in the ϕ-direction are zero the equations become

mass:

$$\rho_t = -(A\rho_y + u\rho_s/\lambda - Bu_y + \rho u_s/\lambda + \rho v_y/\delta + C), \tag{2.5}$$

s-momentum:

$$u_t = -(Au_y + uu_s/\lambda - Bp_y/\rho^2 + p_s/(\rho\lambda) + D), \tag{2.6}$$

y-momentum:

$$v_t = -(Av_y + uv_s/\lambda + p_y/(\delta\rho) - E), \tag{2.7}$$

energy:

$$h_t = -(Ah_y + uh_s/\lambda - p_t/\rho - Ap_y/\rho - up_s/(\rho\lambda)), \tag{2.8}$$

where

$$A = v/\delta - y\delta_t/\delta - uy\mu \tan\beta/(\delta\lambda), \tag{2.9}$$

$$B = \rho y\mu \tan\beta/(\delta\lambda), \tag{2.10}$$

$$C = \rho u \sin\theta/r + \rho v(K/\lambda + \cos\theta/r), \tag{2.11}$$

$$D = Kuv/\lambda, \tag{2.12}$$

$$E = Ku^2/\lambda. \tag{2.13}$$

Here

$$r = y\cos\theta + \int_0^s \sin\theta\, ds \tag{2.14}$$

is the distance from the symmetry axis and

$$K = -\frac{d\theta}{ds} \qquad (K = 1 \text{ for a sphere}), \tag{2.15}$$

$$\lambda = 1 + K\,\delta y, \tag{2.16}$$

$$\mu = 1 + K\delta \tag{2.17}$$

are variables from the coordinate transformation.

All variables appearing in the equations are dimensionless quantities. The relation to dimensional quantities are given by

$$\begin{aligned} s &= s'/R', \\ y &= y'/R', \\ r &= r'/R', \\ p &= p'/(\rho'_\infty V'^2_\infty), \\ h &= h'/V'^2_\infty, \\ \rho &= \rho'/\rho'_\infty, \\ t &= t'V'_\infty/R', \end{aligned}$$

where the subscript ∞ denotes free stream values and the prime denotes dimensional quantities.

The pressure p is introduced as an independent variable instead of ρ by using the relation

$$\rho = \gamma ph/(\gamma - 1), \tag{2.18}$$

where γ is the ratio of specific heats for the gas. The mass equation then becomes

$$p_t = -(Ap_y + up_s/\lambda + a^2(\rho u_s/\lambda - Bu_y + \rho v_y/\delta + C)), \tag{2.19}$$

where

$$a = (p\gamma/\rho)^{1/2} \tag{2.20}$$

is the local speed of sound.

We want the steady-state solution, i.e., a solution to Eqs. (2.6)–(2.8), (2.19) with all time derivatives equal to zero. Writing the dependent variables as a vector

$$w = (u\ v\ h\ p)' \tag{2.21}$$

the equations become

$$L(s, y, w)\, w_s + M(s, y, w)\, w_y + f(s, y, w) = 0, \tag{2.22}$$

where

$$L = \begin{pmatrix} u/\lambda & 0 & 0 & 1/(\rho\lambda) \\ 0 & u/\lambda & 0 & 0 \\ 0 & 0 & u/\lambda & -u/(\rho\lambda) \\ a^2\rho/\lambda & 0 & 0 & u/\lambda \end{pmatrix} \tag{2.23}$$

$$M = \begin{pmatrix} A & 0 & 0 & -B/\rho^2 \\ 0 & A & 0 & 1/\delta \\ 0 & 0 & A & -A/\rho \\ -a^2B & a^2\rho/\delta & 0 & A \end{pmatrix} \tag{2.24}$$

$$f = \begin{pmatrix} D \\ -E \\ 0 \\ a^2C \end{pmatrix} \tag{2.25}$$

Boundary Conditions

We want to solve Eqs. (2.22) in a region between the body and the shock. Then we have physically very natural boundary conditions at the shock and the body. At the shock the values of the variables behind the shock can be calculated from the free stream conditions using the Rankine–Hugoniot relations for a steady shock, when the shock shape is known, i.e., θ and β are known. The Rankine–Hugoniot relations are

$$\begin{aligned} u &= V_\infty \left(\cos(\theta + \beta)\cos\beta + \sin(\theta + \beta)\sin\beta\,\frac{2/m_\infty^2 + \gamma - 1}{\gamma + 1}\right), \\ v &= V_\infty \left(\cos(\theta + \beta)\sin\beta - \sin(\theta + \beta)\cos\beta\,\frac{2/m_\infty^2 + \gamma - 1}{\gamma + 1}\right), \\ p &= p_\infty + 2\rho_\infty V_\infty^2 \sin^2(\theta + \beta)\,\frac{1 - 1/m_\infty^2}{\gamma + 1}, \\ h &= \gamma p\,\frac{2/m_\infty^2 + \gamma - 1}{\rho_\infty(\gamma - 1)(\gamma + 1)}, \end{aligned} \tag{2.26}$$

where

$$m_\infty = M_\infty \sin(\theta + \beta)$$

denotes the free stream component perpendicular to the shock. The connections between δ and β is defined by

$$\frac{d\delta}{ds} = (1 + K\delta)\,\mathrm{tg}\,\beta. \tag{2.27}$$

The only boundary condition at the body is

$$v(s, 0) = 0 \tag{2.28}$$

and at the symmetry line, the conditions are

$$\begin{aligned} u(0, y) &= 0, \\ v_s(0, y) &= 0, \\ h_s(0, y) &= 0, \\ p_s(0, y) &= 0, \\ \delta_s(0) &= 0. \end{aligned} \tag{2.29}$$

The subsonic flow in the stagnation region is followed by a supersonic region further downstream along the body. If the region A extends sufficiently far downstream in the supersonic region, system (2.22) is hyperbolic at the line $s = s_b$ with the s-coordinate being time-like. Therefore no boundary condition shall be given there.

For each given s there are five boundary conditions (2.26) and (2.28), but only four differential equations. However, this is no contradiction, since the unknown function $\delta(s)$ occurs in the coefficients of (2.22). (Also β is unknown, but is related to δ by (2.27).)

3. The Solution Method for Region A

We solve Eqs. (2.22) using finite-difference approximations in region A, which extends sufficiently far into the supersonic region. Therefore we choose a value s_b such that u is greater then the speed of sound, and solve the problem on the rectangle $0 \leqslant s \leqslant s_b$, $0 \leqslant y \leqslant 1$. For most problems there is no difficulty in choosing a proper value of s_b, but we have to check the supersonic condition when the solution is found.

We define a mesh in the rectangle such that the meshpoints are (s_n, y_j), $n = 0,..., N$, $j = 0,..., J$, where $s_n = -\Delta s/2 + n\Delta s$, $y_j = j\Delta y$, and $\Delta s = s_b/(N - 0.5)$, $\Delta y = 1/J$. For functions $f(s, y)$ of s and y, f_{nj} denotes $f(s_n, y_j)$.

We get as unknowns the values of u, v, h, p at each mesh point and the value of δ at s_n, $n = 0,..., N$, thus making a total of $4(N + 1)(J + 1) + N + 1$ unknowns.

The complete difference scheme in region A is defined as follows:

1. Central differences in the interior,

$$L_{nj} \frac{w_{n+1,j} - w_{n-1,j}}{2\Delta s} + M_{nj} \frac{w_{n,j+1} - w_{n,j-1}}{2\Delta y} + f_{nj} = 0.$$

2. Six-point scheme near the body for the u-, h-, and p-equations and at the shock for the p-equation

$$\hat{L}_{nk} \frac{w_{n+1,k} - w_{n-1,k}}{2\Delta s} + \hat{M}_{nk} \frac{w_{nk+1/2} - w_{nk-1/2}}{\Delta y} + \hat{f}_{nk} = 0,$$

where the second subscript $k = \frac{1}{2}, N - \frac{1}{2}$ denotes average values between adjacent points in the y-direction. The caret above L, M, f indicates that the proper rows are deleted.

3. Boundary values $w_{n,J}$ at the shock from (2.26), $\tan \beta$ from central difference approximation of

$$\frac{d\delta}{ds} = (1 + K\delta) \tan \beta.$$

4. Boundary condition at the body,

$$v_{n0} = 0.$$

5. Conditions at the symmetry line,

$$\begin{aligned} u_{1j} + u_{0j} &= 0, \\ v_{1j} - v_{0j} &= 0, \\ h_{1j} - h_{0j} &= 0, \\ p_{1j} - p_{0j} &= 0, \\ \delta_1 - \delta_0 &= 0. \end{aligned}$$

6. Extrapolation at the outflow boundary $s = s_b$,

$$w_{Nj} = 2w_{N-1,j} - w_{N-2,j},$$
$$\delta_N = 2\delta_{N-1} - \delta_{N-2},$$
$$\tan \beta_N = 2\tan \beta_{N-1} - \tan\beta_{N-2}.$$

These approximations are second-order accurate except for the linear extrapolation at the right boundary, but since no boundary conditions *to the differential equations* are approximated there we should still be able to get second-order accuracy in the interior.

Due to the extrapolation of δ, we also have accuracy one order lower in the coefficients one step from the boundary at $s = s_b$. Since this occurs at this coordinate line only, the overall accuracy should not be affected.

We would like to emphasize here the importance of choosing the right boundary conditions at $y = 0$ and $y = 1$. The following table shows the properties of the characteristics (eigenvalues are given in Section 4)

Elliptic part	Hyperbolic part
$y = 0$ parallel to body: 2	parallel to body: 2 pointing out of the domain: 1 pointing into the domain: 1
$y = 1$ pointing into the domain: 2	pointing into the domain: 3 pointing out of the domain: 1

Since part of the hyperbolic domain is included in region A, it is essential that the numerical boundary conditions be properly posed for the difference scheme considered as a marching procedure. Therefore three "extra" boundary conditions are given at $y = 0$, and one "extra" boundary condition at $y = 1$ as specified in part 2 above. If the six-point scheme (which is the type of extra condition used in our case) were used for all four equation at $y = 0$, this would correspond to an underspecification at $y = 0$, and to an overspecification at $y = 1$. Numerical experiments confirm this analysis; oscillations occur in the hyperbolic domain, and they are more severe if region A is extended farther downstream from the sonic line.

It is possible to make an independent computation of the solution at the symmetry line if an estimate of the tangential derivative $\partial u/\partial s$ is available. This solution could then be used as boundary data for the main calculation. Gustafsson and Kreiss [5] have shown that for time-dependent problems such an overspecifying of an artificial boundary leads to slow convergence to the steady state and can also cause oscillations if the given values are not very near the true solution. We have experienced this latter effect also for the steady-state problem when making some test calculations.

We will now describe how the solution to the difference approximation is obtained.

With all unknowns ordered into one vector

$$W = (w'_{11}w'_{21} \cdots w'_{N1}w'_{12} \cdots w'_{N2} \cdots w'_{NJ}\delta_1 \cdots \delta_N)',$$

the equations, which are ordered in a similar manner, give rise to a nonlinear system of equations in the form

$$H(W) \equiv G(W) \cdot W + F(W) = 0. \tag{3.1}$$

Here the equations containing difference quotients have been multiplied by Δy in order to get elements in G of the same order of magnitude.

This system is solved iteratively by Newton's method. All variables, even the δ_n, $n = 1,..., N$, are involved in the iterative process, so that the adjustment of the shock stand-off distance is made automatically by the Newton procedure. The criterion for convergence is that the norm of the residual, $\| H(W)\| = \max_j | H_j(W)|$ be less than some specified value.

The accuracy in the solution can then be estimated from the correction in the last iteration.

The initial approximation required to start the iterative method is obtained in the following way:

1. The shock distance along the body is approximated.

2. The values of u, v, h, and p behind the shock are calculated from the Rankine–Hugoniot conditions using free stream values and the approximation of $\tan \beta$ described above.

3. In the interior the values of u, h, and p are held constant between the shock and the body, while v is interpolated linearly between the shock value and the zero value at the body.

The initial approximation of the shock distance used is the one given by Berman in [1], where an analytical expression for the shock distance is given, which involves only the density ratio ρ_∞/ρ across the shock at the symmetry line.

If a calculation on a coarse mesh has been performed, and we want a calculation made on a finer mesh, then the initial data for the Newton iteration are obtained by linear interpolation from the solution on the coarser mesh.

The Linear System of Equations

The Newton iteration procedure used for solving the nonlinear system of equations (3.1) requires the solution of a system of linear equations for every iteration. The major part of the computing time is spent on these calculations, and the storage requirements for this part tend to grow rapidly when the mesh is refined.

With the ordering of the unknown and of the equations introduced above, the Jacobian of the nonlinear system (3.1) has the structure

$$\frac{\partial H}{\partial W} = \left[\begin{array}{cccc|c} A_1 & B_1 & & & d_1 \\ C_2 & A_2 & B_2 & & d_2 \\ & \ddots & \ddots & & \\ & & \ddots & B_{J-1} & \\ & & C_J & A_J & d_n \\ \hline & & & C_{J+1} & d_{J+1} \end{array}\right] \tag{3.2}$$

This is a sparse matrix, the main part of which is block tridiagonal, However, since the coefficients of the equations are functions of δ and of $\tan \beta$, there are also nonzero elements in the last N columns.

The matrices A_j contain three block diagonals with 4×4 matrices, while B_j, C_j have only one such diagonal. (Due to the boundary approximation A_1, B_1, and C_{J+1} have a somewhat different structure.

The linear system of equations is solved by Gaussian elimination, using row pivoting. The equations are scaled so that the largest elements in all rows are of the same magnitude. The scaling factors are always chosen to be a power of the machine radix, (IBM machines have 16 as radix) so that no round-off error should be caused by the scaling; this type of scaling is recommended by Forsythe and Moler [4].

The method used for the Gaussian elimination is based on algorithms for factorization of band matrices given by Martin and Wilkinson [7], which do not use more storage than is needed for storing the band portion of the matrix plus some extra diagonals needed when pivoting is performed. However, when the mesh is refined, the storage requirements still grow rapidly. For example, 8 times more storage is needed when the step size in each direction is halved. Therefore we have used the method used by Blomster and Sköllermo in the transsonic nozzle flow problem [2], where only a small part of the band portion of the matrix is kept in the main storage at any given time. External storage is then used for the rest of the matrix. This method was modified to suit the special format of matrix (3.2) and to perform row pivoting. A system with the same coefficient matrix and a new right-hand side could be solved rapidly by reading the stored LU-decomposition of the matrix from external storage and performing the back substitutions. This procedure is used for the quasi-Newton's method, where the same Jacobian is used for more than one iteration.

The block diagonals of the system contain many zeros. For example, the average number of nonzero elements in a row is only 15, regardless of the mesh size. The time needed to solve the system depends very much on the rate of fill-in, i.e., the number of zero elements that become nonzero during the elimination procedure. There are pivoting strategies so that the fill-in is held at a minimum or reasonably near it, for example, those given by Tewarson [11]. However, these are based on a rather detailed analysis of submatrices of the original matrix at several stages during the elimination process. We have compared three different procedures.

(a) The elimination is carried out as if all the elements within the band are nonzero.

(b) At the elimination of the jth variable, the zeros in the jth column are taken into consideration.

(c) As in (b) but the zeros of the jth row are also taken into consideration.

For the 7×9 mesh with a total of 259 unknowns and bandwidth of 66, the operation count is

Method (a)	$1140 \cdot 10^3$,
Method (b)	$540 \cdot 10^3$,
Method (c)	$260 \cdot 10^3$.

The differences in efficiency shown by these numbers should be more pronounced for a finer mesh.

Since the matrix (3.2) is very sparse, iterative solution methods could be considered. However, for the transsonic flow problem reported in [2], where the corresponding system has block tridiagonal form, several iterative methods were tried, but none of them was efficient compared to Gaussian elimination. Furthermore, in our case we have the additional difficulty with nonzero columns containing $d_1, d_2, \ldots, d_{J+1}$, and this is not likely to improve the convergence rate for iterative methods.

4. The Marching Procedure in Region B

Equation (2.22) for steady state can be written

$$w_s + Qw_y + g = 0, \tag{4.1}$$

where

$$Q = L^{-1}M = \begin{pmatrix} \left(Au + \frac{Ba^2}{\rho}\right)\alpha & -\frac{a^2}{\delta}\alpha & 0 & -\left(\frac{A}{\rho} + \frac{Bu}{\rho^2}\right)\alpha \\ 0 & \frac{A\lambda}{u} & 0 & \frac{\lambda}{u\,\delta\rho} \\ -\left(A + \frac{Bu}{\rho}\right)a^2\alpha & \frac{ua^2}{\delta}\alpha & \frac{A\lambda}{u} & \left(\frac{Au}{\rho} + \frac{Ba^2}{\rho^2}\right)\alpha - \frac{A\lambda}{\rho u} \\ -(A\rho + Bu)\,a^2\alpha & \frac{ua^2\rho}{\delta}\alpha & 0 & \left(Au + \frac{Ba^2}{\rho}\right)\alpha \end{pmatrix}$$

$$g = L^{-1}f = \begin{pmatrix} (Du - a^2C/\rho)\,\alpha \\ -E\lambda/u \\ (-Da^2 + a^2Cu/\rho)\,\alpha \\ (-Da^2\rho + a^2Cu)\,\alpha \end{pmatrix}$$

$$\alpha = \frac{\lambda}{u^2 - a^2}.$$

If $u > a$ this system is hyperbolic, and a marching procedure can be used. We use the leap-frog scheme with a dissipation term; see, e.g., [3]. To comply with the usual notation for initial-value problems we substitute w_{nj} by w_j^n, etc. The scheme is

$$w_j^{n+1} = w_j^{n-1} - 2\Delta s(QD_0 w_j^n + g_j^n) - \epsilon(\Delta y)^4 (D_+D_-)^2 w_j^{n-1}, \qquad j = 2, 3, \ldots, J-2, \tag{4.2}$$

$$w_j^{n+1} = w_j^{n-1} - 2\Delta s(QD_0 w_j^n + g_j^n) - 4\epsilon(\Delta y)^2 D_+D_- w_j^{n-1}, \qquad j = 1, J-1. \tag{4.3}$$

We have used $\epsilon = 0.01$ throughout the experiments. At the boundary $y = 0$ we use the boundary condition

$$v_0^n = 0,$$

and the variables u, p, h are computed by substituting D_0 by the second-order one-sided operator $D_+(I - 0.5\Delta y D_+)$ in (4.2) and putting $\epsilon = 0$.

To explain the treatment of the boundary $y = 1$, we consider for a moment Eq. (4.1) written in conservation law form

$$W_s + F_{\hat{y}}(W) = 0, \qquad 0 \leqslant \hat{y} \leqslant \delta, \tag{4.4}$$

where $\hat{y}$ denotes the original unscaled coordinate, and where the components of W are nonlinear combinations of u, v, h, p. The position δ of the shock is determined by the Rankine–Hugoniot relations for (4.4),

$$\frac{d}{ds}[W] = -[F]. \tag{4.5}$$

Here [ ] denotes the jump across the shock. In our application, there are three negative and one positive eigenvalues of the Jacobian $\partial F/\partial W$ just inside the shock.

In order to advance the scheme one step at the boundary, we must therefore use one extra boundary condition. By using Eq. (4.5), the five variables u_J^{n+1}, v_J^{n+1}, h_J^{n+1}, p_J^{n+1}, δ^{n+1} then can be determined.

In our setting, Eq. (4.5) is equivalent to (2.26), (2.27), and the difference scheme we get when the trapezoidal rule is used for (2.27)

$$\begin{aligned}
&\text{(a)} \quad u_J^{n+1} = V_\infty[\cos(\theta + \beta^{n+1}) \cos \beta^{n+1} \\
&\qquad + \sin(\theta + \beta^{n+1}) \sin \beta^{n+1}(2/m_\infty^2 + \gamma - 1)/(\gamma + 1)], \\
&\text{(b)} \quad v_J^{n+1} = V_\infty[\cos(\theta + \beta^{n+1}) \sin \beta^{n+1} \\
&\qquad - \sin(\theta + \beta^{n+1}) \cos \beta^{n+1}(2/m_\infty^2 + \gamma - 1)/(\gamma + 1)], \\
&\text{(c)} \quad p_J^{n+1} = p_\infty + 2\rho_\infty V_\infty^2 \sin^2(\theta + \beta^{n+1}) \frac{1 - 1/m_\infty^2}{\gamma + 1}, \\
&\text{(d)} \quad h_J^{n+1} = \gamma p^{n+1} \frac{2/m_\infty^2 + \gamma - 1}{\rho_\infty(\gamma - 1)(\gamma + 1)}, \\
&\text{(e)} \quad \frac{\delta^{n+1} - \delta^n}{\Delta s} = \frac{1}{2}[\operatorname{tg} \beta^n(1 + K^n\delta^n) + \operatorname{tg} \beta^{n+1}(1 + K^{n+1}\delta^{n+1})].
\end{aligned} \tag{4.6}$$

The computational procedure is:

(1) Compute p_J^{n+1} by the extrapolation

$$p_J^{n+1} = 2p_{J-1}^n - p_{J-2}^{n-1}.$$

(2) Compate β^{n+1} from Eq. (4.6c).

(3) Compute u_J^{n+1}, v_J^{n+1}, h_J^{n+1} from (4.6a), (4.6b), (4.6d).

(4) Compute δ^{n+1} from (4.6e).

The eigenvalues of Q are

$$\tau_{1,2} = A\lambda/u,$$

$$\tau_{3,4} = \alpha\left(uA + \frac{Ba^2}{\rho} \pm \left(\left(uA + \frac{Ba^2}{\rho}\right)^2 + \frac{1}{\alpha}\left(\frac{a^2}{\delta^2} + \frac{a^2B^2}{\rho^2} - A^2\right)\right)^{1/2}\right),$$

where τ_4 corresponding to the minus sign is the positive eigenvalue at $y = 1$.

Let $W = (W^{(1)}, W^{(2)}, W^{(3)}, W^{(4)})^T$ denote the characteristic variables such that the homogeneous system (4.1) with constant coefficients takes the form

$$W_s + \begin{pmatrix} \tau_1 & & & \\ & \tau_2 & & \\ & & \tau_3 & \\ & & & \tau_4 \end{pmatrix} W_y = 0,$$

where $W = T^{-1}w$, $T^{-1}QT = \operatorname{diag}(\tau_1, \tau_2, \tau_3, \tau_4)$.

After transformation conditions (4.6a), (4.6b), (4.6d) can be written

$$\begin{pmatrix} W^{(1)} \\ W^{(2)} \\ W^{(3)} \end{pmatrix} = \begin{pmatrix} S^{(1)}W^{(4)} \\ S^{(2)}W^{(4)} \\ S^{(3)}W^{(4)} \end{pmatrix} + \begin{pmatrix} G^{(1)} \\ G^{(2)} \\ G^{(3)} \end{pmatrix}, \qquad y = 1,$$

which is the correct form for a well-posed problem. $W^{(4)}$ at $y = 1$ is necessarily dependent on values computed inside the domain, since the corresponding characteristic is going out of the domain. p, which is extrapolated in our scheme, is the fourth component of TW, and therefore we must make sure that $W^{(4)}$ is included in the expression for p. In other words, the fourth component of the eigenvector corresponding to τ_4 must be nonzero.

Assume that this is not the case, i.e., the eigenvector has the form $x = (x_1, x_2, x_3, 0)^T$. Then the second equation of the system

$$(Q - \tau_4 I)\, x = 0 \tag{4.7}$$

is

$$(A\lambda/u - \tau_4)\, x_2 = 0.$$

Since

$$\tau_1 = \tau_2 = A\lambda/u \neq \tau_4$$

x_2 must be zero. But then the first equation of (4.7) implies $x_1 = 0$, and finally the third equation implies $x_3 = 0$. Therefore, we have proved that x_4 is nonzero.

The implementation of the algorithm is as follows.

The condition on the starting value $s = s_b$ is

$$u(s_b, y) > a(s_b, y), \qquad 0 \leqslant y \leqslant 1,$$

and the solutions obtained from method A at $s = s_b$ are used as initial values. The first step is generated by using a forward difference in the s-direction. The initial step size is computed from

$$\Delta s = 0.8\Delta y / \max_{\nu, y} |\tau_\nu(s_b, y)|, \tag{4.8}$$

which guarantees that the von Neumann condition for (4.2), (4.3) is satisfied for ϵ of the order 0.01; see [3]. The largest possible step size is thus computed every kth step, where $k = 5$ is a typical value. The step size is increased, only if it can be doubled, otherwise the old one is used. If the step size must be decreased, it is halved.

The variable step size is an important part of the algorithm, since close to the sonic line the eigenvalues τ_3, τ_4 are large in magnitude. In the applications presented in this paper, the Mach number will increase with increasing s, i.e., $|\tau_3|$, $|\tau_4|$ will get smaller. Therefore the step size need seldom be decreased.

The reason for changing the step size only when it can be doubled is made clear by studying a simple model example.

Consider the ordinary differential equation

$$u_s = i\omega u,$$

which is obtained by Fourier transforming $u_s = u_y$. The leap-frog scheme is

$$v^{n+1} = v^{n-1} + 2hiv^n, \qquad h = \omega\Delta s,$$

which has the solution

$$v^n = \sigma_1\kappa_1{}^n + \sigma_2\kappa_2{}^n,$$

where

$$\kappa_1 = ih + (1 - h^2)^{1/2},$$

$$\kappa_2 = ih - (1 - h^2)^{1/2}.$$

At a certain step the step size is changed to

$$\Delta\hat{s} = (2 - \alpha)\,\Delta s, \qquad 0 \leqslant \alpha < 1,$$

and the new solution is defined by

$$\hat{v}^n = \hat{\sigma}_1 \hat{\kappa}_1{}^n + \hat{\sigma}_2 \hat{\kappa}_2{}^n,$$

where

$$\hat{\kappa}_1 = (2 - \alpha)\, ih + (1 - (2 - \alpha)^2\, h^2)^{1/2},$$

$$\hat{\kappa}_2 = (2 - \alpha)\, ih - (1 - (2 - \alpha)^2\, h^2)^{1/2}.$$

The second part of $\hat{v}^n$ is the parasitic solution, which has an oscillating character, and therefore we want to keep $\hat{\sigma}_2$ as small as possible. Assume that $\hat{v}^1 = v^m$, and that $\hat{v}^0$ is obtained by linear interpolation

$$\hat{v}^0 = \alpha v^{m-1} + (1 - \alpha)\, v^{m-2},$$

which corresponds to the new step size $\Delta\hat{s} \cdot \hat{\sigma}_1$, $\hat{\sigma}_2$ are determined by

$$\hat{\sigma}_1 + \hat{\sigma}_2 = \alpha(\sigma_1 \kappa_1^{m-1} + \sigma_2 \kappa_2^{m-1}) + (1 - \alpha)(\sigma_1 \kappa_1^{m-2} + \sigma_2 \kappa_2^{m-2}),$$

$$\hat{\kappa}_1 \hat{\sigma}_1 + \hat{\kappa}_2 \hat{\sigma}_2 = \sigma_1 \kappa_1{}^m + \sigma_2 \kappa_2{}^m$$

and we get

$$\hat{\sigma}_2 = (\hat{\kappa}_2 - \hat{\kappa}_1)^{-1} \{\sigma_1 \kappa_1{}^m (1 - [\alpha \kappa_1^{-1} + (1 - \alpha)\, \kappa_1^{-2}]\, \hat{\kappa}_1) + \sigma_2 \kappa_2{}^m (1 - [\alpha \kappa_2^{-1} + (1 - \alpha)\, \kappa_2^{-2}]\, \hat{\kappa}_1)\}.$$

For small h-values we have

$$\kappa_1^{-1} = 1 - ih - \frac{h^2}{2} + \mathcal{O}(h^3),$$

$$\kappa_1^{-2} = 1 - 2ih - 2h^2 + \mathcal{O}(h^3),$$

$$\kappa_2^{-1} = 1 - ih + \frac{h^2}{2} + \mathcal{O}(h^3),$$

$$\kappa_2^{-2} = 1 + 2ih - 2h^2 + \mathcal{O}(h^3),$$

$$\hat{\kappa}_1 = 1 + (2 - \alpha)\, ih - \frac{(2 - \alpha)^2}{2} h^2;$$

hence

$$\hat{\sigma}_2 = -\frac{1}{2} \left\{ \sigma_1 \kappa_1{}^m \left[\left(\frac{(2 - \alpha)^2}{2} - \frac{4 - 3\alpha}{2} \right) h^2 + \mathcal{O}(h^3) \right] + \sigma_2 \kappa_2{}^m [2\alpha + \mathcal{O}(h)] \right\}.$$

Since $\sigma_1 = \mathcal{O}(1)$, $\sigma_2 = \mathcal{O}(h^2)$, we get

$$\hat{\sigma}_2 = \mathcal{O}(h^3) \qquad \text{for } \alpha = 0,$$

$$= \mathcal{O}(h^2) \qquad \text{for } \alpha > 0.$$

Therefore, the coefficient for the oscillating part is made as small as possible with the choice $\alpha = 0$, i.e., when the step size is doubled.

5. Numerical Results

The numerical method was programmed and run on the IBM 370/158 computer at the Uppsala University Computing Center. The solution is uniquely defined by the geometry of the body, the free stream Mach number M_m and by γ. Two types of bodies have been studied; one half sphere, which could be followed by an afterbody, and one spherically capped cone. Three different Mach numbers have been used, $M_m = 2, 10, 40$. $\gamma = 1.4$ is used for all cases. (see Figs. 3–6.)

The same step size in the y-direction is used for both regions A and B. In the s-direction the step size required by the marching procedure in region B is in general smaller than the one used in region A. The solution in region B is therefore interpolated to obtain the values at equally spaced points in the whole region. To get a continuous representation for graphical output, these values are finally interpolated using cubic splines.

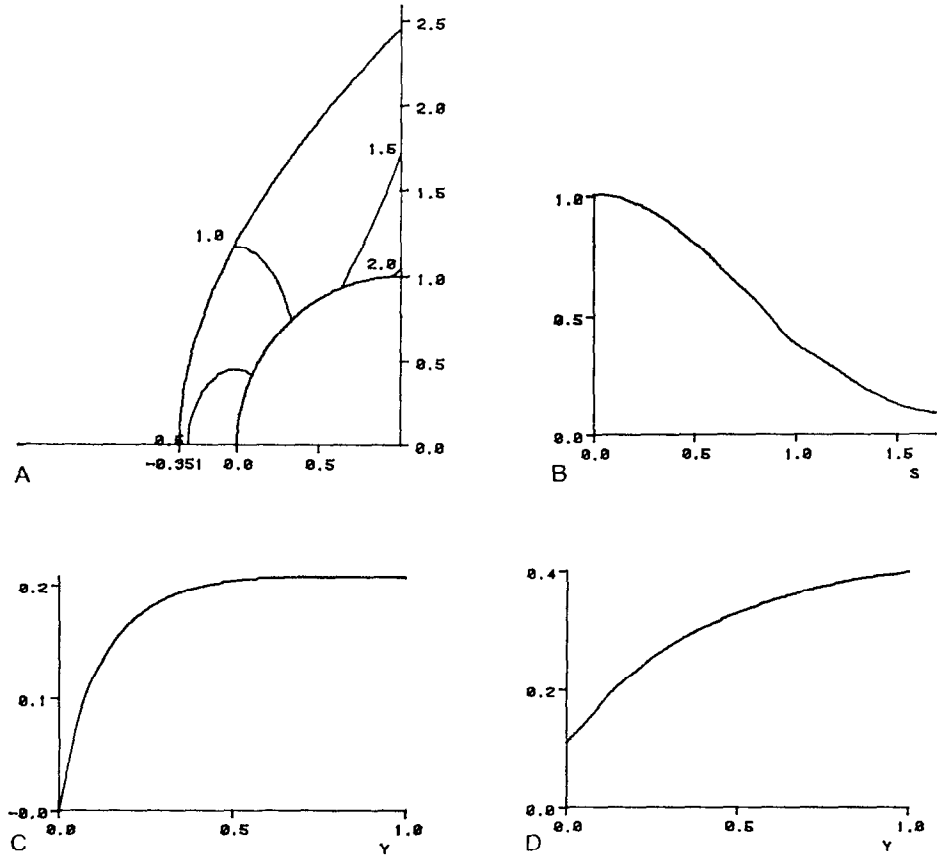

FIG. 3. Result from half-sphere, Mach 2. (A) Shock shape and Mach lines, (B) pressure along body, (C) v—velocity at $s = 1.57$, (D) pressure at $s = 1.57$.

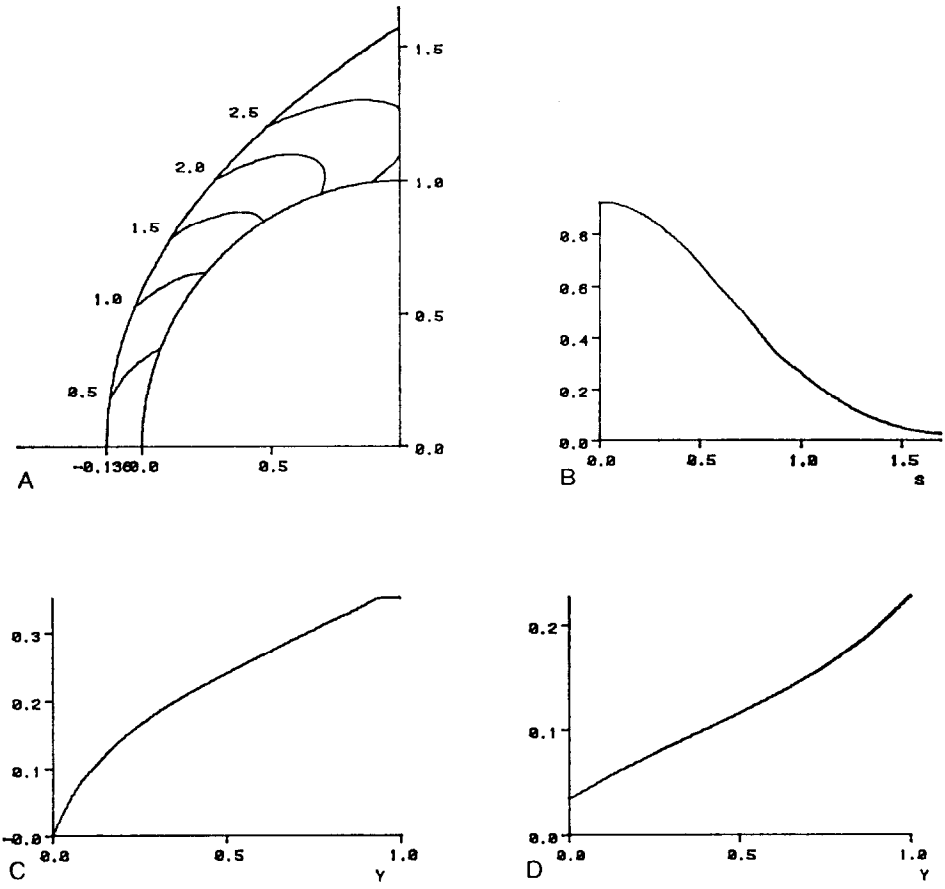

FIG. 4. Result from half-sphere, Mach 10. (A) Shock shape and Mach lines, (B) pressure along body, (C) v-velocity at $s = 1.57$, (D) pressure at $s = 1.57$.

The efficiency of the algorithm depends essentially on the convergence property of the Newton iterations. It turns out that the largest change in the solution occurs in the first iteration, and therefore the Jacobian is recomputed only once. In this way we have been able to obtain an accuracy of the order 10^{-4} (more precise $\| H(W)\| \approx 10^{-4}$) in five iterations and still keep the total computing time low.

We have run many more cases than those which are presented here. In all cases where the solution is such that it is possible to define the region A so that the whole subsonic region is included, convergence was obtained, and the whole computation procedure was behaved well as described above. (Actually we got convergence also in cases where the outflow boundary was partly subsonic.) In particular it is worth noting that the way of defining the initial data always gives a converging iteration process. In general the whole solution method seems to be very reliable.

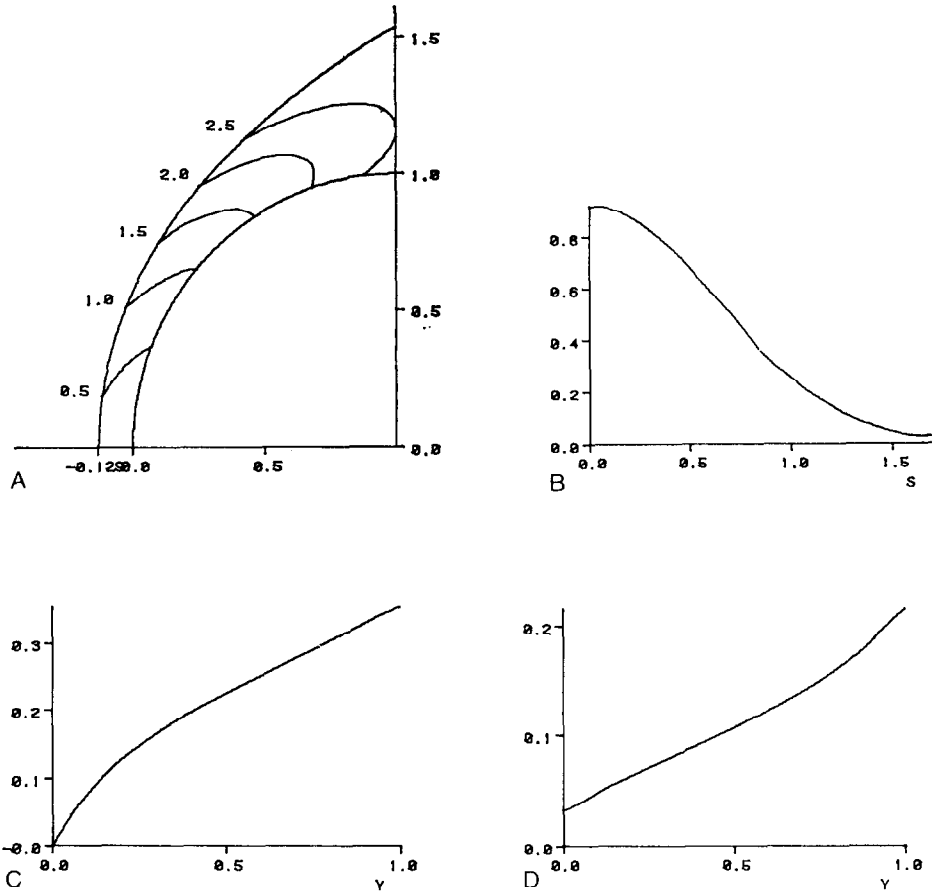

Fig. 5. Result from half-sphere, Mach 40. (A) Shock shape and Mach lines, (B) pressure along body, (C) v—velocity at $s = 1.57$, (D) pressure at $s = 1.57$.

For each case the results are presented in four figures. The first shows the shock shape and lines of constant Mach number. The second shows the pressure along the body. The third and the fourth show the velocity components and the pressure at the outflow boundary. In all cases 17 mesh-points were used in the y-direction in both regions A and B. For Mach number 2, 11 mesh-points were used in the s-direction in region A; the corresponding number of mesh-points for Mach numbers 10 and 40 was 10. The computing time for a half-sphere at $M_\infty = 10$ was, for our computer,

Newton procedure	116 sec
Marching procedure (85 steps)	17 sec
Total	133 sec

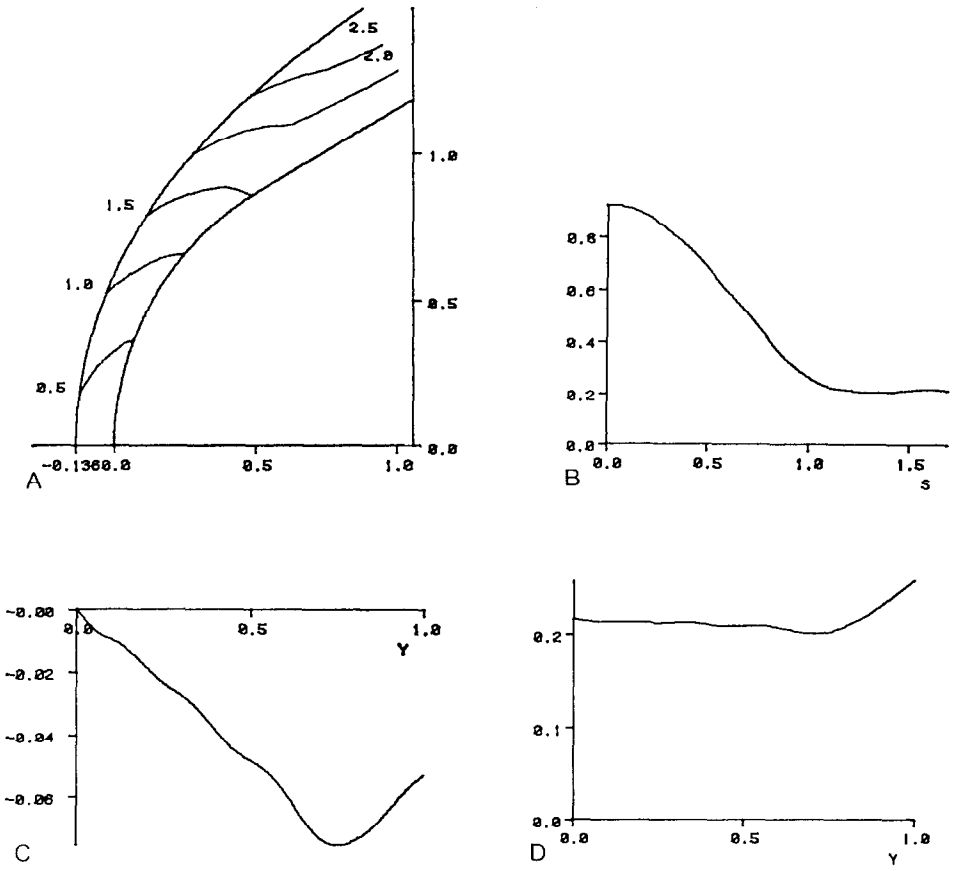

FIG. 6. Result from spherically capped cone, half top angle 30°, Mach 10. (A) Shock shape and Mach lines, (B) pressure along body, (C) v—velocity at $s = 1.65$, (D) pressure at $s = 1.65$.

REFERENCES

1. R. J. BERMAN, *AIAA J.* **3** (1965), 778–780.
2. J. BLOMSTER AND G. SKÖLLERMO, "Finite Difference Computation of Steady Transsonic Nozzle Flow," Report No. 66, Department of Computer Sciences, Uppsala University, 1977.
3. B. ENGQUIST, B. GUSTAFSSON, AND J. VREEBURG, *J. Comput. Phys.* **27** (1978), 295–314.
4. G. FORSYTHE AND G. MOLER, "Computer Solutions of Linear Algebraic Systems," Prentice–Hall, Englewood Cliffs, N. J., 1967.
5. B. GUSTAFSSON AND H.-O. KREISS, *J. Comput. Phys.* **30** (1979), 333–351.
6. H. LOMAX AND M. INOUYE, "Numerical Analysis of Flow Properties about Blunt Bodies Moving at Supersonic Speed in an Equilibrium Gas," TR R-204, NASA, Washington, D. C., 1964.
7. R. S. MARTIN, J. H. WILKINSON, *in* "Handbook for Automatic Computation," Vol. II, pp. 70–92, Springer–Verlag, Berlin/Heidelberg, 1971.

8. A. W. RIZZI AND M. INOUYE, *AIAA J.* **11** (1973), 1478–1485.
9. A. W. RIZZI, *in* "Proceedings, Conference on Numerical Methods in Applied Fluid Dynamics, Reading, Mass., January 4–6, 1978."
10. K. SUTTON, "Characteristics of Coupled Nongray Radiating Gas Flow with Ablation Product Effects about Blunt Bodies during Planetary Entries," Doctorial thesis, North Carolina State University, Raleigh, 1973.
11. R. P. TEWARSON, "Sparse Matrices," Academic Press, New York, 1973.